International Journal of Mechanical, Industrial and Aerospace Sciences
ISSN: 2517-9950
Vol:4, No:5, 2010

Identification of an Mechanism Systems by Using the Modified PSO Method

Chih-Cheng Kao Hsin- Hua Chu

***Abstract*—**This paper mainly proposes an efficient modified particle swarm optimization (MPSO) method, to identify a slider-crank mechanism driven by a field-oriented PM synchronous motor. In system identification, we adopt the MPSO method to find parameters of the slider-crank mechanism. This new algorithm is added with "distance" term in the traditional PSO's fitness function to avoid converging to a local optimum. It is found that the comparisons of numerical simulations and experimental results prove that the MPSO identification method for the slider-crank mechanism is feasible.

***Keywords*—**Slider-crank mechanism, distance, system identification, modified particle swarm optimization.

I. Introduction

A slider-crank mechanism is widely used in gasoline and diesel engines, and has been studied extensively in the past three decades. The responses of the system found by Viscomi and Ayre [1] are to be dependent upon the five parameters as the length, mass, damping, external piston force and frequency. The steady-state responses of the flexible connecting rod of a slider-crank mechanism with time-dependent boundary effect were obtained by Fung [2]. A slider-crank mechanism with constantly rotating speed was controlled by Fung et al. [3], where the system is actuated by a field-oriented control permanent magnet (PM) synchronous servomotor.

Particle swarm optimization (PSO) is a stochastic population based optimization approach, and was first published by Kennedy and Eberhart in 1995 [5,6]. PSO has been shown to be an efficient, roust and simple optimization algorithm. In this paper, a modified PSO algorithm is proposed to improve the searching ability and prevent from being trapped in a local optimum. The main difference of the MPSO from the PSO is its fitness function considers the "distance" to avoid converging to a local optimum. From these empirical studies it can be concluded that the MPSO is sensitive to control parameter choices.

This study successfully demonstrates that the dynamic formulation can give a wonderful interpretation of a slider-crank mechanism in comparison with the experimental results. Furthermore, a new identified method using the MPSO is proposed, and it is confirmed that the method can perfectly searches the parameters of the slider-crank mechanism driven by a servomotor through the numerical simulations and experimental results.

Chih-Cheng Kao is with the Department of Electrical Engineering, Kao-Yuan University, Kaohsiung 821, Taiwan, R.O.C. (corresponding author to provide phone: 886-7-607-7013; fax: 886-7-607-7009; e-mail: cckao@cc.kyu.edu.tw).
Hsin- Hua Chu is graduate student of the Department of Electrical Engineering, Kao-Yuan University, Kaohsiung 821, Taiwan, R.O.C.

II. Dynamic modeling

Figure 1 shows the physical model of a slider-crank mechanism, where the mass center and the radius of the rigid disk are denoted as point "O" and length "r", respectively. And "l" is denoted as the length of the connected rod AB. The angle θ is between OA and the X-axis, while the angle ϕ is between the rod AB and the X-axis. In OXY plane, the geometric positions of gravity centers of rigid disk, connected rod, and slider, respectively, are as follows:

$$x_{1cg} = 0, \quad y_{1cg} = 0 \tag{1}$$

$$x_{2cg} = r\cos\theta + \frac{1}{2}l\cos\phi, \quad y_{2cg} = \frac{1}{2}l\sin\phi \tag{2}$$

$$x_{3cg} = r\cos\theta + l\cos\phi, \quad y_{3cg} = 0. \tag{3}$$

The mechanism has a constrained condition as follows

$$r\sin\theta = l\sin\phi. \tag{4}$$

The angle ϕ can be found from Eq. (4) as

$$\phi = \sin^{-1}\left(\frac{r}{l}\sin\theta\right). \tag{5}$$

By taking account of the control force and constraint force, the equation in the matrix form can be obtained as

$$\mathrm{M}(\mathbf{Q})\ddot{\mathbf{Q}} + \mathrm{N}(\mathbf{Q},\dot{\mathbf{Q}}) + \Phi_{\mathbf{Q}}{}^{T}\boldsymbol{\lambda} = \mathbf{Q}^{\mathbf{A}} \tag{6}$$

where $\mathbf{M(Q)}$, $\mathbf{N(Q,\dot{Q})}$, $\boldsymbol{\Phi}_{\mathbf{Q}}^{\mathbf{T}}\boldsymbol{\lambda}$ and $\mathbf{Q}^{\mathbf{A}}$ can be seen in the Appendix A.

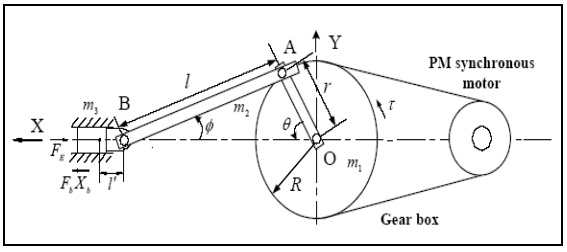

Fig. 1 The physical model of a slider-crank mechanism

2.2 Decouple the differential equations

In the dynamic analysis, the partitioning method [3,4] is employed, and the partitioning coordinate vector is selected as

$$\mathbf{Q} = [\mathbf{Q}_1 \quad \mathbf{Q}_2 \cdots \quad \mathbf{Q}_3]^T = [\mathbf{p}^T \quad \mathbf{q}^T]^T \tag{7}$$

where $\mathbf{p} = [p_1 \quad p_2 \cdots \quad p_m]^T$ and $\mathbf{q} = [q_1 \quad q_2 \cdots \quad q_k]^T$ are the m dependent and k independent coordinates, respectively. The m constraint equations are

$$\mathbf{\Phi(Q)} \equiv \mathbf{\Phi}(\mathbf{p}, \mathbf{q}) = \mathbf{0}. \tag{8}$$

Numerical method may be used to solve the set of nonlinear algebraic equation (8). If the m constraint equations are independent, the existence of a solution **p** for a given **q** can be asserted by an implicit function theory.

Decomposing **Q** into **p** and **q**, the system equations become

$$\mathrm{M}^{\mathbf{pp}}\ddot{\mathbf{p}} + \mathrm{M}^{\mathbf{pq}}\ddot{\mathbf{q}} + \Phi_{\mathbf{p}}{}^{T}\boldsymbol{\lambda} = \mathbf{Q}^{\mathbf{p}} - \mathrm{N}^{\mathbf{p}} \tag{9a}$$

$$\mathrm{M}^{\mathbf{qp}}\ddot{\mathbf{p}} + \mathrm{M}^{\mathbf{qq}}\ddot{\mathbf{q}} + \Phi_{\mathbf{q}}{}^{T}\boldsymbol{\lambda} = \mathbf{Q}^{\mathbf{q}} - \mathrm{N}^{\mathbf{q}} \tag{9b}$$

$$\Phi_{\mathbf{p}}\ddot{\mathbf{p}} + \Phi_{\mathbf{q}}\ddot{\mathbf{q}} = \boldsymbol{\gamma} \tag{9c}$$

By using equations (9a) and (9c) and eliminating $\boldsymbol{\lambda}$ and $\ddot{\mathbf{p}}$ yields

$$\boldsymbol{\lambda} = \left(\Phi_{\mathbf{p}}{}^{T}\right)^{-1}\left[\mathbf{Q}^{\mathbf{p}} - \mathrm{N}^{\mathbf{p}} - \mathrm{M}^{\mathbf{pp}}\ddot{\mathbf{p}} - \mathrm{M}^{\mathbf{pq}}\ddot{\mathbf{q}}\right] \tag{10}$$

$$\ddot{\mathbf{p}} = \mathbf{\Phi}_{\mathbf{p}}{}^{-1}\left[\boldsymbol{\gamma} - \mathbf{\Phi}_{\mathbf{q}}\ddot{\mathbf{q}}\right] \tag{11}$$

Equations (9b), (10) and (11) can be combined in the matrix form as

$$\hat{\mathbf{M}}(\mathbf{q})\ddot{\mathbf{q}} + \hat{\mathbf{N}}(\mathbf{q}, \dot{\mathbf{q}}) = \hat{\mathbf{F}} \tag{12}$$

where

$$\begin{aligned}\hat{M} &= \mathrm{M}^{\mathbf{qq}} - \mathrm{M}^{\mathbf{qp}}\Phi_{\mathbf{p}}{}^{-1}\Phi_{\mathbf{q}} \\ &\quad - \Phi_{\mathbf{q}}{}^{T}\left(\Phi_{\mathbf{p}}{}^{T}\right)^{-1}\left[M^{\mathbf{pq}} - M^{\mathbf{pp}}\Phi_{\mathbf{p}}{}^{-1}\Phi_{\mathbf{q}}\right]\end{aligned} \tag{13}$$

$$\begin{aligned}\hat{N} &= \left[\mathbf{N}^{\mathbf{q}} - \mathbf{\Phi}_{\mathbf{q}}{}^{T}\left(\mathbf{\Phi}_{\mathbf{p}}{}^{T}\right)^{-1}\mathbf{N}^{\mathbf{p}}\right] \\ &\quad + \left[\mathrm{M}^{\mathbf{qp}}\Phi_{\mathbf{p}}{}^{-1} - \Phi_{\mathbf{q}}{}^{T}\left(\Phi_{\mathbf{p}}{}^{T}\right)^{-1}\mathrm{M}^{\mathbf{pp}}\Phi_{\mathbf{p}}{}^{-1}\right]\gamma\end{aligned} \tag{14}$$

$$\hat{F} = \mathbf{Q}^{\mathbf{q}} - \Phi_{\mathbf{q}}{}^{T}\left(\Phi_{\mathbf{p}}{}^{T}\right)^{-1}\mathbf{Q}^{\mathbf{p}}. \tag{15}$$

Equation (12) is a set of differential equations with only one independent generalized coordinate vector $\mathbf{q} = [\theta]$. It is seen that the entries of $\hat{\mathbf{M}}$, $\hat{\mathbf{N}}$ and $\hat{\mathbf{F}}$ of Eq. (12) has two independent variables θ and ϕ. By using Eq. (4) and its time derivative, we could derive the equation with only one independent variable θ as follows

$$\hat{M}(\theta)\ddot{\theta} + \hat{N}(\theta, \dot{\theta}) = \hat{F}(\theta) \tag{16}$$

where

$$\begin{aligned}\hat{M} &= \left[(2m_3 + m_2) + \frac{m_3}{c}r\cos\theta\right]\left(\frac{r^3}{c}\cos\theta\sin^2\theta\right) \\ &\quad + (m_2 + m_3)r^2\sin^2\theta \\ &\quad + \frac{1}{3}m_2\left(\frac{l}{c}\right)^2(r\cos\theta)^2 + \frac{1}{2}m_1r^2 + J_m,\end{aligned} \tag{17}$$

$$\begin{aligned}\hat{N} &= \left\{m_2 r^2\sin\theta\cos\theta\left[1 - \frac{l^2}{3c^2} + \frac{r}{c}\cos\theta\right.\right. \\ &\quad \left.\left. + \frac{(lr)^2}{3c^4}\cos^2\theta + \frac{r^3}{2c^3}\cos\theta\sin^2\theta\right]\right. \\ &\quad - m_2\frac{r^3}{2c}\sin^3\theta + m_3 r^2\sin\theta\cos\theta \\ &\quad \left[1 - \frac{r^2}{c^2}\sin^2\theta + \frac{r^2}{c^2}\cos^2\theta + \frac{2r}{c}\cos\theta\right. \\ &\quad \left. + \frac{2r}{c}\cos\theta\frac{r^4\cos^2\theta\sin^2\theta}{c^4} + \frac{r^3}{c^3}\sin^2\theta\cos\theta\right] \\ &\quad \left. - m_3\frac{r^3}{c}\sin^3\theta\right\}\dot{\theta}^2 + B_m\dot{\theta} + \frac{1}{2}m_2 gr\cos\theta,\end{aligned} \tag{18}$$

$$\hat{F} = K_t i_q - (F_B + F_E)r\sin\theta\left(1 + \frac{r}{c}\cos\theta\right),$$

$$c = \sqrt{l^2 - r^2\sin^2\theta} \tag{19}$$

The system becomes an initial value problem and can be directly integrated by using the fourth order Runge-Kutta method.

III. Modified Particle Swarm Optimization

3.1 Particle swarm optimization

Birds (particles) flocking optimizes a certain objective function in a PSO system. Each agent knows its best value so far (*pbest*) and its position. This information is analogy of personal experiences of each agent. Moreover, each agent knows the best value so far in the group (*gbest*) among *pbests*. This information is analogy of knowledge of how the other agents around them have performed. The PSO concept [5-6] consists of changing the velocity of each particle toward its *pbest* and *gbest* locations. In the PSO, each particle moves to a new position according to new velocity and the previous positions of the particle. This is compared with the best position generated by previous particles in the fitness function, and the best one is kept; so each particle accelerates in the direction of not only the local best solution but also the global best position. If a particle discovers a new probable solution, other particles will move closer to it to explore the region more completely in the process.

In general, there are three attributes, current position x_j, current velocity v_j and past best position $pbest_j$, for particles in the search space to present their features. Each particle in the swarm is iteratively updated according to the aforementioned attributes. For example [5-11], the *j*th particle is represented as $x_j = (x_{j,1}, x_{j,2}, \ldots, x_{j,g})$ in the g-dimensional space. The best previous position of the *j*th particle is recorded and represented as $pbest_j = (pbest_{j,1}, pbest_{j,2}, \ldots, pbest_{j,g})$. The index of best particle among all particles in the group is represented by the $gbest_g$. The rate of the position change (velocity) for particle *j* is represented as $v_j = (v_{j,1}, v_{j,2}, \ldots, v_{j,g})$. The modified velocity and position of each particle can be calculated using the current velocity and distance from $pbest_{j,g}$ to $gbest_{j,g}$ as shown in the following formulas[11]:

$$v_{j,g}^{(t+1)} = w \cdot v_{j,g}^{(t)} + c_1 Rand() \cdot (pbest_{j,g}^{(t)} - x_{j,g}^{(t)}) + c_2 Rand^{*}() \cdot (gbest_{j,g}^{(t)} - x_{j,g}^{(t)}),$$
$$x_{j,g}^{(t+1)} = x_{j,g}^{(t)} + v_{j,g}^{(t+1)}. \quad (20)$$
$$j = 1,2,\cdots,n; g = 1,2,\cdots,m$$

where n is the number of particles in a group; m is the number of members in a particle; t is the pointer of iterations (generations); $v_{j,g}^{(t)}$ is the velocity of the particle j at iteration t, $V_g^{\min} \le v_{j,g}^{(t)} \le V_g^{\max}$; w is the inertia weighting factor; c_1, c_2 are the acceleration constants; *Rand*(), *Rand**() are random numbers between 0 and 1; $x_{j,g}^{(t)}$ is the current position of particle j at iteration t; $pbest_j$ is the *pbest* of particle j; $gbest_g$ is the *gbest* of the group g.

In the above procedures, the parameter $V_g^{\max}$ determine the resolution or fitness, with which regions are searched between the present position and the target position. If $V_g^{\max}$ is too high, particles might fly past good solutions. If $V_g^{\max}$ is too low, particles may not explore sufficiently beyond local solutions.

The constants c_1 and c_2 represent the weighting of the stochastic acceleration terms that pull each particle toward pbest and gbest positions. Low values allow particles to roam far from the target regions before being tugged back. On the other hand, high values result in abrupt movement toward or past target regions.

Suitable selection of inertia weighting factor w provides a balance between global and local explorations, thus requiring less iteration on average to find a sufficiently optimal solution. As originally developed, w often decreases linearly from about 0.9 to 0.4 during a run. In general, the inertia weighting factor w is set according to the following equation [6][9]:

$$w = w_{\max} - \frac{w_{\max} - w_{\min}}{iter_{\max}} \times iter \quad (21)$$

where $iter_{\max}$ is the maximum number of iterations (generations), and $iter$ is the current number of iterations.

3.2 Modified particle swarm optimization

The main point of the MPSO differs from the PSO is to consider the "distance" in its fitness function to avoid converging to a local optimum. Assign a rank (i.e., the number place 1, 2, 3, …, etc.) RE_k to the calculated error of each new individual, v_k, $k = 1,\cdots,PS$, PS is the population size. A combined population with $2 \times PS$ individuals is formed. Unlike previously developed statistic methods, the concept of "distance" is added to the fitness function to prevent from being trapped in a local minimum. The fitness score of the kth individual is modified by [12,13]

$$F_k = RE_k + \rho \times RD_k, \quad k = 1,\cdots,2 \times PS. \quad (22)$$

where ρ is an adaptive decay scale, $\rho_{\max}$ is set as 0.7 and $\rho_{\min}$ is set as 0.005 in this paper. RD_k is the rank of D_k assigned to the kth individual, where D_k is the distance from the individual to the current best solution vector, and is given by

$$D_k = \left\| v_k - v_{best} \right\| \quad (23)$$

where v_k is the vector of the kth individual in the combined population, and v_{best} is the current best solution vector.

An adaptive scheme is defined as [12]

$$\rho_\Delta = R \times (\rho_{\max} - \rho_{\min}) / g_{\max} \quad (24)$$

$$\rho(g+1) = \begin{cases} \rho(g) - \rho_\Delta, & F_{\min}(g) = F_{\min}(g-1) \\ \rho(g), & F_{\min}(g) < F_{\min}(g-1) \end{cases} \quad (25)$$

and

$$\rho(g+1) = \rho_{\min};\ \text{if}\ \rho(g) - \rho_\Delta < \rho_{\min} \quad (26)$$

where ρ_Δ is the step size; $F_{\min}$ is the minimum value of fitness functions; R is the regulating scale and is set as 1.25 in this paper, and $g_{\max}$ is the maximum allowable number of iterations.

Individuals will be ranked in ascending according to their fitness scores by a sorting algorithm. The *PS* individuals are transcribed along with their fitness for the next generation. If the new population does not include the current best solution, the best solution must be replaced with the last individual in the new population. In addition, a gradually decreased decay scale can satisfy a successive statistic searching process by first using the diversification (bigger ρ) to explore more regions, and then the intensification (smaller ρ) to exploit the neighborhood of an elite solution. The current best solution (point *A*) for a minimum fitness problem as shown in the Fig. 2 may not reach the global optimum [12,13], and there are three electable solutions exist. Generally, solutions with slightly better fitness (point *C* or *B*) prevailed, so the solution trapped into the valley prematurely. The more attractive solution (point *G*) is relatively far away from point A, but it nears the global optimal. To prevent prematurity, point *G* with slightly worse fitness than *C*, it needs a higher rank to be selected. That is, a higher RD_k is awarded to a longer D_k.

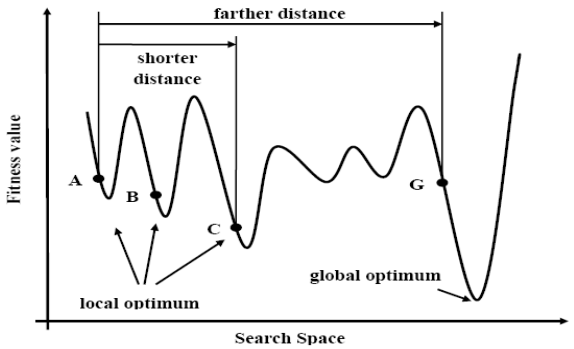

Fig. 2 The concept of distances

Stopping Criteria: Stopping criteria is given in the following order:

1) maximum allowable number of iterations reached.

2) number of iterations reached without improving the current best solution.

Fig. 3 shows the flow chart of the proposed algorithm.

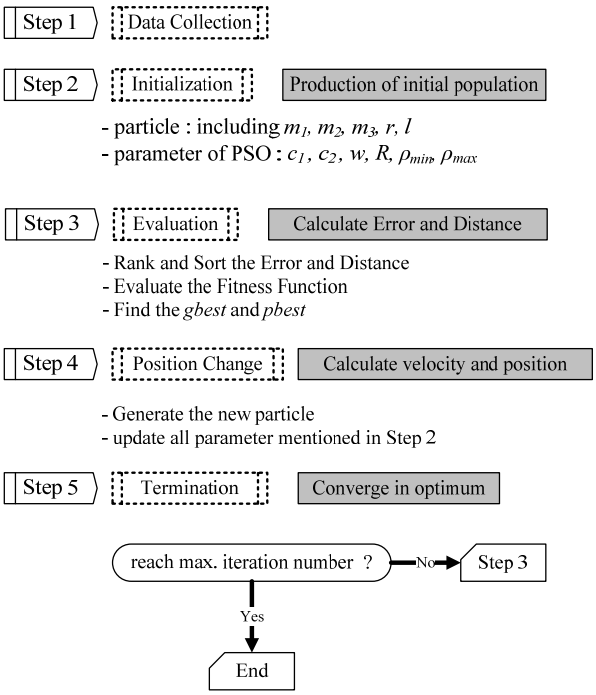

Fig. 3 The flow chart of the MPSO

3.3 Parameter identifications

How to define the fitness function is the key point of the MPSO, since the fitness function is a figure of merit, and could be computed by using any domain knowledge. In this paper, we adopt the fitness function as follows [14,15]:

$$F(parameters) = \sum_{i=1}^{n} E_i^2 \tag{27}$$

$$E_i = x^{(i)} - x^{*(i)} \tag{28}$$

where n is the total number of samples and E_i is the calculated error of the i th sampling time, $x^{*(i)}$ is a solution by using the fourth-order Runge-Kutta method to solve the dynamic Equations (12) for the PM synchronous servomotor drive coupled with a slider-crank mechanism with the parameters identified from these two methods, and $x^{(i)}$ is the displacement measured experimentally at the i th sampling time.

IV. Comparisons between PSO and MPSO methods

The physical model of the slider-crank mechanism driven by a servomotor. In the parameter identification, we utilize the MPSO and PSO methods to identify the 5 parameters m_1 、 m_2 、 m_3 、 r and l simultaneously, and the fitness function is described as Eq. (27). The identified results are given in Table1.

TABLE I
The identified parameters of the numerical simulations

Parameter	$m_1\ (kg)$	$m_2\ (kg)$	$m_3\ (kg)$	$r\ (m)$	$l\ (\mathrm{m})$
Feasible domain	0.000~1.000	0.000~1.000	0.000~1.000	0.000~1.000	0.000~1.000
The actual value	0.232	0.332	0.600	0.030	0.217
The identified value of the PSO method	0.311	0.304	0.752	0.024	0.325
The identified value of the MPSO method	0.234	0.331	0.603	0.030	0.216

Figure 4 shows the convergence characteristics in PSO and MPSO methods of the slider-crank mechanism system. It is seen from Fig. 4 that the proposed MPSO method is superior to the PSO method.

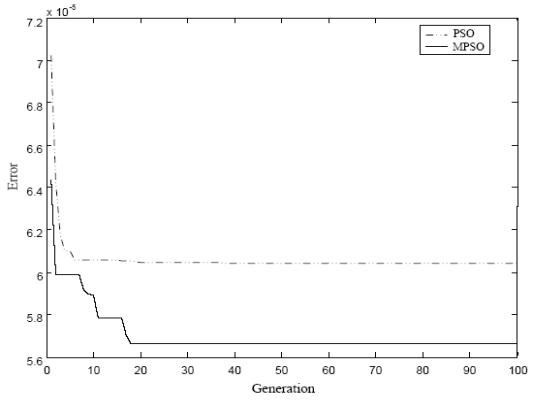

Fig. 4 Comparison of convergence characteristics in PSO and MPSO methods of the slider-crank mechanism system

V. Conclusions

The dynamic formulations of a slider-crank mechanism driven by a field-oriented PM synchronous motor have been successfully formulated with only one independent variable. Furthermore, the main objective of this study is to utilize PSO and MPSO methods to identify a slider-crank mechanism driven by a servomotor. According to the comparisons between identified results and displacement errors, it is found that MPSO method has the best matching with the

experimental results.

It is concluded that the implementations of MPSO are different from the PSO in five aspects. Firstly, its fitness function considers the distance to avoid converging to a local optimum. Secondly, for the MPSO, vectors with good enough fitness scores would be used as candidates to create new solutions. Thirdly, it has the advantage of the MPSO to conquer various constraints without using the fitness function with penalties, and can perform better. Fourthly, the solution is coded with a decimal representation, and saves computer memory. Finely, the gradually decaying parameters can satisfy a successive statistic searching process by first using the diversification (bigger parameters) to reserve the larger attractive region. Then, the intensification (smaller parameters) used to search the small neighborhood of an elite solution.

APPENDIX A

We can obtain the Euler-Lagrange equation as follows

$$\mathbf{M}(\mathbf{Q})\ddot{\mathbf{Q}} + \mathbf{N}(\mathbf{Q},\dot{\mathbf{Q}}) + \mathbf{\Phi}_{\mathbf{Q}}{}^{T}\boldsymbol{\lambda} = \mathbf{Q}^{\mathbf{A}}$$

where

$$\mathbf{M} = \begin{bmatrix} A & E \\ E & B \end{bmatrix}, \qquad \mathbf{N} = \begin{bmatrix} K_W \\ P_W \end{bmatrix}$$

and

$$A = \frac{1}{3}m_2 l^2 + m_3 l^2 \sin^2\phi,$$

$$B = \frac{1}{2}m_1 r^2 + (m_2 + m_3) r^2 \sin^2\theta,$$

$$E = \left(\frac{1}{2}m_2 + m_3\right) r\, l \sin\theta \sin\phi,$$

$$K_W = m_3 l^2 \dot{\phi}^2 \sin\phi \cos\phi + \left(\frac{1}{2}m_2 + m_3\right) r\, l \dot{\theta}^2 \cos\theta \sin\phi + \frac{1}{2}m_2 g\, l \cos\phi$$

$$P_W = \left(\frac{1}{2}m_2 + m_B\right) r\, l \dot{\phi}^2 \sin\theta \cos\phi + (m_2 + m_B) r^2 \dot{\theta}^2 \sin\theta \cos\theta.$$

$$\mathbf{Q}^{\mathbf{A}} = \begin{bmatrix} (F_E + F_B) l \sin\phi \\ (F_B + F_E) r \sin\theta - \tau \end{bmatrix}$$

$$\mathbf{\Phi}_{\mathbf{Q}} = \left[\frac{\partial \mathbf{\Phi}(\mathbf{Q})}{\partial \mathbf{Q}}\right] = \begin{bmatrix} -l\cos\phi & r\cos\theta \end{bmatrix}$$

and $\boldsymbol{\lambda}$ is the Lagrange multiplier.

REFERENCES

[1] Viscomi, B. V., and Arye, R. S., "Nonlinear Dynamic Response of Elastic Slider-Crank Mechanism" ASME J. of Eng. for Industry, Vol. 93, pp. 251-262, 1971.

[2] Fung, R. F., "Dynamic Response of the Flexible Connecting Rod of a Slider-Crank Mechanism with Time-Dependent Boundary Effect" Computer & Structure, 63, No. 1,pp. 79-90, 1997.

[3] Fung, R. F., Lin, F. J., Huang, J. S. and Wang, Y. C., "Application of Sliding Mode Control with a Low-pass Filter to the Constantly Rotating Slider-Crank Mechanism" The Japan Society of Mechanical Engineers, C, 40, No. 4, pp 717-722, 1997.

[4] Lin, F. J., Fung, R. F., and Lin, Y. S., "Adaptive Control of Slider-Crank Mechanism Motion: Simulation and Experiments", International Journal of System Science, 28, No. 12, pp. 1227-1238, 1997.

[5] Kennedy, J., Eberhart, R. C., "Particle Swarm Optimization", Proceedings of the IEEE International Joint Conference on Neural Networks, IEEE Press, pp. 1942-1948, 1995.

[6] Eberhart, R. C., Kennedy, J., "A New Optimizer Using Particle Swarm Theory", Proceedings of the Sixth International Symposium on Micromachine and Human Science, Nagoya, Japan, pp.39-43, 1995.

[7] Wu, S. L. and Lin, S. K., 1997, "Implementation of damped-rate resolved-acceleration robot control," *Control Engineering Practice*, Vol. 5, No. 6, pp. 791-800.

[8] Campa, R., Kelly, R. and Garcia, E., 2001, "On stability of the resolved acceleration control," *In Proc. 2001 IEEE Int. Conf. On Robotics and Automation*, pp. 3523-3528.

[9] Kennedy, J., "The Particle Swarm: Social Adaptation of Knowledge", Proceedings of the IEEE International Conference on Evolutionary Computation, Indianapolis, USA, pp. 303-308, 1997.

[10] Naka, S., Genji, T., Yura, T., Fukuyama, Y., "A Hybrid Particle Swarm Optimization for Distribution State Estimation", IEEE Transactions on Power systems Vol. 18, No.1, pp.60-68, 2003.

[11]Shi, Y., Eberhart, R.C. ," Empirical Study of Particle Swarm Optimization ",Proceedings of the IEEE Congress on Evolutionary Computation, IEEE Press, pp.1945-1950, 1999.

[12] Lin, W. M., Cheng, F. S., and Tsay, M. T., "Nonconvex Economic Dispatch by Integrated Artificial Intelligence", IEEE Transactions on Power systems, Vol. 16, No. 2, pp. 307-311, 2001.

[13] Lin, W. M., Cheng, F. S., and Tsay, M. T., "An Improved Tabu Search for Economic Dispatch With Multiple Minima", IEEE Transactions on Power systems, Vol. 17, No. 1, pp. 108-112, 2002.

[14] Zhang, X., Huang, Y., Liu, J., Wang, X., and Gao, F., "A Method Identifying the Parameters of Bouc-Wen Hysteretic Nonlinear Model Based on Genetic Algorithm", Intelligent Processing Systems, pp. 602-605, 1997.

[15] Ha, J. L., Kung, Y. S., Fung, R. F., and Hsien, S. C., "A Comparison of Fitness Functions for the Identification of Piezoelectric Hysteretic Actuator Based on the Real-Coded Genetic Algorithm", Sensors and Actuators , Vol.132, pp.643-650, 2006.